



HAL
open science

Evaluating Different Strategies to Minimize cold-start Emissions from Gasoline Engines in steady-state and Transient Regimes

Shreya Nandi, C. Chaillou, Christophe Dujardin, Pascal Granger, Emmanuel Laigle, André Nicolle, Caroline Norsic, Melissandre Richard

► **To cite this version:**

Shreya Nandi, C. Chaillou, Christophe Dujardin, Pascal Granger, Emmanuel Laigle, et al.. Evaluating Different Strategies to Minimize cold-start Emissions from Gasoline Engines in steady-state and Transient Regimes. *Topics in Catalysis*, 2022, *Topics in Catalysis*, 66, p.13-14. 10.1007/s11244-022-01721-3 . hal-04047740

HAL Id: hal-04047740

<https://hal.univ-lille.fr/hal-04047740v1>

Submitted on 17 Apr 2024

HAL is a multi-disciplinary open access archive for the deposit and dissemination of scientific research documents, whether they are published or not. The documents may come from teaching and research institutions in France or abroad, or from public or private research centers.

L'archive ouverte pluridisciplinaire **HAL**, est destinée au dépôt et à la diffusion de documents scientifiques de niveau recherche, publiés ou non, émanant des établissements d'enseignement et de recherche français ou étrangers, des laboratoires publics ou privés.

Evaluating different strategies to minimize cold-start emissions from gasoline engines in steady-state and transient regimes

Shreya Nandi^a, Christophe Chaillou^b, Christophe Dujardin^a, Pascal Granger^a, Emmanuel Laigle^b, André Nicolle^b, Caroline Norsic^c, Melissandre Richard^{a*}

^a Univ. Lille, CNRS, Centrale Lille, Univ. Artois, UMR 8181 – UCCS – Unité de Catalyse et Chimie du Solide, F-59000, Lille, France

^b Aramco Fuel Research Center, 232 Avenue Napoleon Bonaparte, 92852, Rueil-Malmaison, France

^c EMC France, 4 Allée de la rhubarbe, Acheres, 78260, France

*Corresponding author: melissandre.richard@centralelille.fr

Author ORCID numbers

S. Nandi: [0000-0002-5904-0539](https://orcid.org/0000-0002-5904-0539)

C. Chaillou: [0000-0001-5292-7463](https://orcid.org/0000-0001-5292-7463)

C. Dujardin: [0000-0001-8266-0165](https://orcid.org/0000-0001-8266-0165)

P. Granger: [0000-0002-8333-4246](https://orcid.org/0000-0002-8333-4246)

E. Laigle: [0000-0003-4951-083X](https://orcid.org/0000-0003-4951-083X)

A. Nicolle : [0000-0002-9234-3101](https://orcid.org/0000-0002-9234-3101)

C. Norsic: [0000-0002-6904-4509](https://orcid.org/0000-0002-6904-4509)

M. Richard: [0000-0001-6789-6997](https://orcid.org/0000-0001-6789-6997)

Statements and Declarations

The authors have no relevant financial or non-financial interests to disclose. The datasets generated during and/or analysed during the current study are available from the corresponding author on reasonable request.

Author contributions

All authors contributed to the study conception and design. Data collection were performed by Shreya Nandi. Shreya Nandi, Christophe Dujardin, Pascal Granger and Melissandre Richard participated to the method development and data analysis. The first draft of the manuscript was written by Shreya Nandi and Melissandre Richard. All authors commented on previous versions of the manuscript. All authors read and approved the final manuscript.

Acknowledgements

This work was supported by ARAMCO Company. The authors thank the Region “Hauts-de-France”, Centrale Lille Institute, the Ministère de l’Enseignement Supérieur et de la Recherche (CPER IRENE and CPER ECRIN) and the European Fund for Regional Economic Development for their support.

Supplementary Data

Supplementary material related to this article can be found in separate document (online version)

Abstract

Exhaust car emissions increase significantly at particular gasoline engine driving cycle such as cold-start when the three-way catalyst has not reached its light-off temperature. More efficient technologies are needed to reduce these extra emissions. This study focuses on comparing two strategies to lower cold-start pollutants on a commercial monolithic catalyst: (i) a high content of PGMs (Pd and Rh) loading with a variable concentration distribution along the catalyst, called zone-coating, was investigated in order to take advantages of an *in situ* pre-heating due to exothermic oxidation processes. And (ii) the use of external device for heating the monolith with the aim to shorten the laps of time to reach the required temperature for their conversion. Both approaches were compared below 300 °C in terms of NO, CO and hydrocarbons conversions as well as N₂O formation with respect to homogeneously wash-coated catalyst. For evaluation, complex exhaust gas compositions were considered at different steady-state air-to-fuel λ ratios and high frequency transient lean/rich regime to mimic real operation in gasoline engine exhaust. Results show that a pre-heating of the catalyst at 300 °C is necessary to avoid completely N₂O formation from NO reduction with CO. Remarkably higher NO and CH₄ conversions were observed during transient regimes rather than steady-state lean, rich or stoichiometric conditions at 200 °C and 300 °C.

Keywords Three-way catalysis, Cold-start emission, Monolithic catalyst, Pre-heating strategy, Transient conditions

1. Introduction

Road transport is a significant contributor to air pollution. Exhaust gas pollutants, carbon monoxide (CO), nitrogen oxides (NO_x) and unburned hydrocarbons (HC) are mainly emitted from the gasoline-based engine tailpipes [1, 2]. Since decades, following ever stricter worldwide regulations on emissions such as Euro 6d, China 6a or US standards, Three-Way Catalysis (TWC) has been implemented to provide an effective solution to the simultaneous abatement of these three pollutants near stoichiometric λ air-to-fuel ratio using commercial catalysts installed in the car engines [3, 4]. These solid materials exhibit complex elemental composition. The active phase is provided by Platinum Group Metals (PGMs) from which palladium and platinum are mainly used for CO and HC oxidation to carbon dioxide and water while rhodium ensured NO_x reduction to molecular nitrogen [5]. A variable PGM loading with flow axial coordinate called zoning or zone-coating is sometimes considered by car manufacturers in order to take advantages of the oxidation reaction exothermicity [6, 7]. Zone-coated configuration was firstly envisaged to segregate metals in order to avoid inactive alloy formation [8]. Then, a high PGM loading in a short front zone of the catalyst was proven to maintain sufficient amount of active sites and thus good conversion performance in close-coupled operation in which particle sintering is favored due to high temperature. On the contrary, the lower temperature downstream allows preserving a high metal dispersion and thus a lower PGM loading [9]. Metal active phase is typically supported on multiple washcoat layers deposited on monolithic-shaped cordierite substrates. Monolith ceramic materials offer good mass and heat transfers, thermal and mechanical stabilities as well as low pressure drop compared to conventional powder catalyst [10–12]. The washcoat layers are commonly composed of a mixture of metallic oxides, namely, γ -alumina due to its high surface area and thermal stability properties [13–15] and ceria-zirconia mixed oxide for its oxygen storage capacity (OSC) [16–18]. Several promoters among rare earth (La, Y, Nd, Pr, Sm) and alkaline (Ba, Sr) elements of the periodic table are then found to further improve OSC and thermal stability performances of the catalyst [19–22].

However, the upcoming regulations feature more stringent emissions limits (Euro 7), thereby getting closer to a zero-emission mobility goal including even regulations on nitrous oxide, ammonia and methane levels. Moreover, the new emission thresholds would be applied at the most polluting driving stage such as cold-starts (including short trips, stop-and-go) or hard accelerations [1, 23]. Among latter, lowering the total pollutant emission during the engine cold start is one of the greatest challenges in exhaust after-treatment as catalysts have not reached their light-off temperature yet, normally around 250–300 °C for TWC [24, 25]. To this end, the development of more efficient technologies is needed to specifically reduce these emissions.

In this work, two different strategies will be evaluated for potentially lowering cold-start emissions that can be applied on to a monolithic catalyst. The first strategy comprises of introducing a very high PGM loading of close to 2 wt.%Pd along the entire catalyst or only in the front zone of the monolith (zone-coating), which can facilitate an *in situ* preheating by promoting an exothermic process from oxidation reactions. The second approach involves an assisted pre-heating of the catalyst using an electric heating device near the light-off temperatures. While most previous studies focused on pre-heating and zone-coating impacts on HC conversion, no dedicated study on N₂O formation has been performed [1, 7, 26]. In preliminary work [27], catalytic efficiencies of zone-coated and homogeneous catalysts in model reactions of CO and C₃'s oxidation or NO reduction were compared regarding to

their detailed washcoat composition, reducibility and surface properties. Quite distinct air-to-fuel regimes ($\lambda=0.5, 1, 1.5$) were evaluated showing that the amount of dopants and PGM should be judiciously dosed to allow pollutant abatement in a cost-effective manner. Herein, the efficiency of the zone-coated strategy is newly discussed compared to a pre-heating step in terms of pollutant conversion and N_2O formation below 300 °C. Interestingly, this evaluation is performed by employing a complex gas mixture of pollutants consisting of CO, NO and various HC introduced simultaneously under different lean/rich/stoichiometric steady-state stages ($\lambda=0.98, 1, 1.02$ respectively) as well as under realistic transient condition (1s lean/rich) in order to mimic the actual operative conditions as prevalent in gasoline engines.

2. Materials and Method

2.1. Monolithic catalyst and its characterizations

The investigated monolith purchased from a leading car manufacturer is hereafter called Monolith-A following confidentiality reasons. Monolith-A results from a zoning with the front side (1/3) having a higher concentration of Palladium while the back side (2/3) is richer in Rhodium. Here, we will study three cases of this fresh catalyst as represented in Figure 1: (i) Monolith-A-full refers to the full catalyst with zoning directly sampled from the commercial exhaust catalyst, (ii) Monolith-A-front, refers to the front side composition only and (iii) Monolith-A-back, refers to the back side composition only. The two latter catalysts are cut accordingly in order to have similar full (void+solid) volumes in each case ($\approx 7.7 \text{ cm}^3$). The specifications of the monolithic catalysts and the methods used for its characterization are detailed elsewhere [27]. Briefly, Monolith-A chemical composition, textural and structural properties have been evaluated using X-Ray Fluorescence (XRF), X-ray Photoelectron Spectroscopy (XPS), Induced Coupled Plasma – Optical Emission Spectroscopy (ICP-OES), Scanning Electronic Microscopy (SEM) as well as N_2 -physisorption analysis.

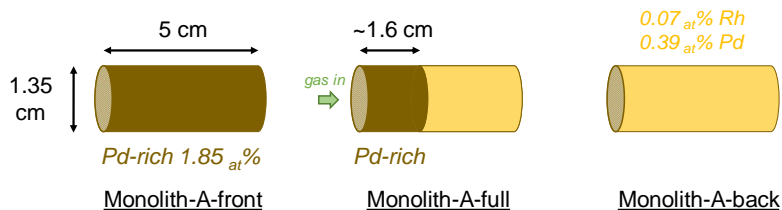


Fig. 1 Schematic representation of monoliths tested with regard to their metal concentrations and distributions along the catalyst

2.2. Catalytic performance measurements

The catalytic test setup has already been described in [27]. In this catalytic performance measurements, a complex mixture of gases composed of CO, CO_2 , NO, O_2 , H_2 and various hydrocarbons has been sent to the monolithic catalyst mimicking the realistic exhaust gas mixture as produced by multiple Euro6d temp gasoline engines as shown in Table 1 below under rich, lean or stoichiometric regimes.

Table 1 Concentration of the realistic mixture gas composition for catalytic performance evaluation at different richness

Mixture	Lean ($\lambda=0.98$) ppm	Stoichiometric ($\lambda=1.00$) ppm	Rich ($\lambda=1.02$) ppm
<i>Main pollutants</i>			
NO	1000	1000	1000
CO	9640	9640	9640
CH ₄	191	191	191
C ₂ H ₂	94	94	94
C ₃ H ₆	478	478	478
n-C ₅ H ₁₂	498	498	498
i-C ₅ H ₁₂	489.5	489.5	489.5
<i>Catalyst inhibitor</i>			
CO ₂	10% _v	10% _v	10% _v
<i>Others</i>			
O ₂	1.70% _v	1.66% _v	1.63% _v
H ₂	3342	3342	3342
He	Balance	Balance	Balance

The air factor (λ) values varied in the range of 0.98–1.02 to illuminate each regime’s significance for a specific reaction with a total flow of 2 L min⁻¹ (at 20 °C, 1 atm) and a space velocity (GHSV) of 42 000 h⁻¹ considering the solid volume only (2.85 cm³). The protocol for the catalytic performance testing is described in Fig S1. The catalysts were firstly degreened for 4 h at 500 °C under oxidative flow (10% O₂/10% H₂O/He). During the catalytic tests, the experimental protocol consisted of 3 isothermal steps at every 100 °C from 100 to 300 °C, where the following regimes switch, lean, rich and stoichiometric change every 15 min after thermal stabilization (Figure S1(b)). The switch regime refers to the periodic 1s transient between rich and lean modes. The gas phase composition at the reactor outlet was analyzed overall using Infrared spectroscopy (IGS Antaris™, Thermo Scientific) and micro-gas chromatography (μ GC double channel, Varian 490), simultaneously.

Pre-heating experiments were performed by previously increasing the temperature of the catalysts under O₂/He flow at every 50 °C from 100 °C to 400 °C before exposure to the complex gas mixture described above. The evolution of reactant and product concentration, especially NO conversion and N₂O formation were followed for 15 min under the 1s lean/rich transient regime at each temperature interval. Last experiment was performed by heating the catalysts directly to 300 °C under the O₂/He mixture before exposure to the full mixture. In that case, different air-to-fuel ratios were examined in the following order: rich1/switch1/rich2/lean/stoichiometric/switch2.

3. Results and discussion

3.1. Catalyst description

The investigated catalyst including the front and the back sides was characterized in detail in reference [27] for morphological, structural, chemical and surface properties. Only the salient features are briefly stated in this paper as follows,

- i. Monolith-A consists of double-washcoat layers over the honeycomb cordierite support with hexagonal channels (800 cpsi) and an open frontal area of 63%.

- ii. It comprises different washcoat elements such as Ce, Zr and Al, including promoters like La, Nd, Pr, S, Ba and Y in varied concentrations across the first and second washcoat layers.
- iii. The Ce/Zr ratio controlling the OSC properties of the catalysts is 0.38 in Monolith-A-front and 0.23 in Monolith-A-back. The front side presents a higher Ce^{3+}/Ce^{4+} surface ratio equivalent to 0.31, indicating higher presence of oxygen vacancies across this zone.
- iv. Washcoats were mainly prepared with blends of metal oxides like alumina and/or ceria-zirconia to provide high specific surface areas and OSC properties, respectively. The first washcoat layer comprises Zr-enriched ceria-zirconia with segregated particles of alumina, which helps minimize the sintering effect at higher operating temperatures. The second layer is made of γ -alumina with segregated particles of ceria-zirconia that helps preserve the alumina phase.
- v. Promoters like La, Nd, Pr and Y are added in small amounts to the washcoat in order to provide thermal stability and enhance OSC properties of the ceria-zirconia. Previous studies on this catalyst confirmed the presence of sulfur stabilized as barium sulfate for the specific role of enhancing HC oxidation and reducing coking effects.
- vi. The zoning strategy applied to the monolith is reflected in the variable concentration of the active metal sites or PGMs across length. The Pd-rich front consists of relatively high concentration (1.85 at.%) of Pd and only 0.01 at.% Rh to assist oxidation reactions, while the Rh-rich back side comprises of 0.07 at.% Rh and only 0.39 at.% of Pd to promote the NO reduction reaction (Figure 1). The latter percentages are given taking into account all the sample (cordierite support and washcoat). Interestingly, a non-uniform Pd axial distribution along the monolith showed better catalytic performances towards hydrocarbon and NO_x conversion as well as a higher temperature profile at the monolith inlet compared to a homogeneously Pd-loaded catalyst (with the same total loading of Pd) [7, 26]. No segregated radial distribution of PGMs was observed within the washcoat layers of Monolith-A.

3.2. Catalytic performance evaluation at low temperature

3.2.1. Zone coating investigation: effect of high Pd content

The effect of the zoning strategy on catalytic performances at low temperature has been investigated in full catalyst as well as its different parts (Pd rich front and Rh-rich back) considering them as individual and distinct catalysts. The aim is to determine the add value of the existing concentration gradients to improve oxidative and reductive properties during the competitive reactions taking place during cold start conditions in the temperature range of 100-300 °C. For that purpose, Monolith-A is exposed to a realistic gas mixture under different regimes periodically, namely, switch, rich, lean and stoichiometric conditions at every 100 °C. Figure 2 focuses on the oxidative properties from the outlet concentration profiles of CO, propene and methane as well as the reduction properties from the NO_x profile and consequent N_2O formation.

The concentration of CO shown in Figure 2(a) during the catalytic performance testing is obviously an outcome of two competing reactions, CO oxidation by oxygen versus that by NO. We can see that at 100 °C none of the CO is oxidized and the concentration profile is unaffected by the subjected regimes. However, as the temperature increases from 100 to 200°C, we can reach full conversion of CO for each of the tested catalysts. The Monolith-A-full and

Monolith-A-front present identical CO profiles and reach 50 % conversion at $T_{50\%}=167$ °C then full conversion at around 150°C. Monolith-A-back present slightly lower activity achieving complete removal of CO only at 210°C with a $T_{50\%}$ observed at 186 °C. Moreover, no effect of the different air-to-fuel ratio is detected overall the entire temperature range. Similar observations can be made in the case of propene conversion depicted in Figure 2(b) for which full conversion is reached at lower temperature for Monolith-A-full and Monolith-A-front at around 182 °C, compared to Monolith-A-back (220 °C). It is clear that higher CO and propene oxidation in the full and front catalysts is a result of higher Pd content in them compared to the back side achieved as a result of the zoning strategy. Interestingly, the trends for Monolith-A-full and Monolith-A-front are almost identical while the high Pd content is only localized in the one third front part of the full catalyst. Finally, it is worthwhile to note that CO and propene conversion are delayed on Monolith-A-back which emphasize the peculiar role of palladium for oxidation reactions.

According to Figure 2(c), methane conversions reaching up to 70% at 300°C in case of Monolith-A-full and Monolith-A-front which is a considerably lower temperature considering methane difficult activation [28]. Monolith-A-back shows lower activity with only 30% of converted methane at 300°C owing to lower concentration of Pd. This is also the case at a lower temperature of 200°C, where methane oxidation starts to a small extent for full and front catalyst unlike the back part. A slight overconcentration of CH₄ can be observed around 150 °C when propene and others hydrocarbons as well as H₂ start to be converted (see Figure S2(f)). The CO₂ concentration simultaneously increases in the same temperature range due to oxidation reactions (Figure S2(d)). The monolith zoning strategy thereby seems to be beneficial in case of efficient conversion of methane to CO₂. Here also, as was the case for CO and propene, a longer Pd-rich zone such as in Monolith-A-front did not result in an improved CH₄ conversion.

The NO_x outlet concentration profiles are presented in Figure 2(d) with N₂O formation profile in Figure 2(e). Here, no nitrous oxide was formed during the progress of this entire reaction for Monolith-A front and back while a trace amount of NO₂ (≈20 ppm) arises above 100 °C for the full catalyst (Figure S2(e)). The presence of ammonia was detected in IR gas analysis during the course of the experiment (Figure S3). However, the nitrogen mass balance does not show any significant deviation associated with the fact that ammonia would not be quantified. It seems obvious that the absence of water in the inlet exhaust, avoiding reforming reactions, is a crucial parameter which likely explain the absence of significant production of ammonia. Much higher NO_x conversion up to 60% is observed for Monolith-A-back at 200°C in the transient mode due to high Rh content (0.09 at.%) along the overall catalyst, suggesting that NO_x reduction at lower temperature would be improved by a higher Rh concentration. This activity could be even positively impacted by the high dispersion and oxidation state of Rh as well as their interaction with the ceria-zirconia washcoat layer despite a low Ce/Zr ratio of 0.23 [29–31]. In case of the rich, lean and stoichiometric steady-state regimes at 200°C the three catalysts show comparable extent of NO_x conversion. On reaching 300°C, Monolith-A-front shows better NO_x conversion due to higher Pd content (1.9 at.%) under the rich, lean and stoichiometric regimes indicating that at medium temperature range higher Pd concentration aids in improving the reduction of NO [9, 32–34]. It is also worth to correlate the high NO_x conversion at 300 °C with the absence of oxygen (Figure S2g). Indeed, O₂ becomes fully converted in reaction of HC oxidation, leaving NO as the only oxidant species remaining in the gas mixture, thus favoring its reactivity and dissociation on Pd. That can

explain the slightly better NO conversion at 300 °C especially in rich and stoichiometric media for all the catalysts. Interestingly, better or almost complete NO_x removal takes place under the switch regime in each catalyst case at 200 °C and 300 °C, respectively compared to the other modes. Similar to the case of methane oxidation, transient conditions seem to assist in improving the catalytic performances for NO_x reduction to nitrogen. Formation of ammonia, in a small extent, was also observed during this transient stage (Figure S3), while no N₂O was formed. The investigated catalysts are clearly more sensitive to the oxygen content or the steady-state regime conditions especially at high temperature with higher activity in the rich conditions while lower activity is observed in lean condition, as expected. The formation of N₂O was also analyzed during the course of this reaction (Figure 2(e)), with its maximum formation in case of Monolith-A-front reaching 50 ppm at 100°C and least amount of N₂O was produced in case of the Monolith-A-back thanks to its higher Rh concentration. In all cases, the highest level of N₂O is formed during the rise of temperature from 100 to 200°C, once again highest for Monolith-A-front reaching a 250 ppm spike. The volume concentration of N₂O formed per minute during the experiment was calculated by integration of its concentration evolution between 100 and 300 °C around 41, 59 and 19 ppm for full, front and back monolithic materials, respectively. Evidently, the higher concentration of Rh is highly beneficial for low temperature NO reduction as well as lowering the extent of N₂O formation, although to only a small extent.

The temperature profiles of outlet gases during catalytic tests on Monolith-A were compared to a blank experiment on Figure S4 in supporting material. A difference of around +40 °C was observed at both 200 °C and 300 °C temperature stages attributed to exothermic HC oxidation reaction taking place in this range. However, no significant deviation was observed between the catalytic tests on Monoliths-A-full, -front and -back. This result indicates that the *in situ* preheating expected from the zone-coating strategy by taking advantages of exothermic process of HC oxidation reaction remains in fact very limited.

At this point one can consider that the zoning strategy helps to partly combine the advantageous effects of higher Rh as well as Pd concentrations to have overall improvement on NO_x reduction properties. In general, in all cases, the Monolith-A-front does not show any remarkable improvement in order to lower cold-start emission in spite of the highest Pd concentration throughout its length. In the next part of the study, we therefore focus on Monolith-A-full and Monolith-A-back only applying a totally different strategy.

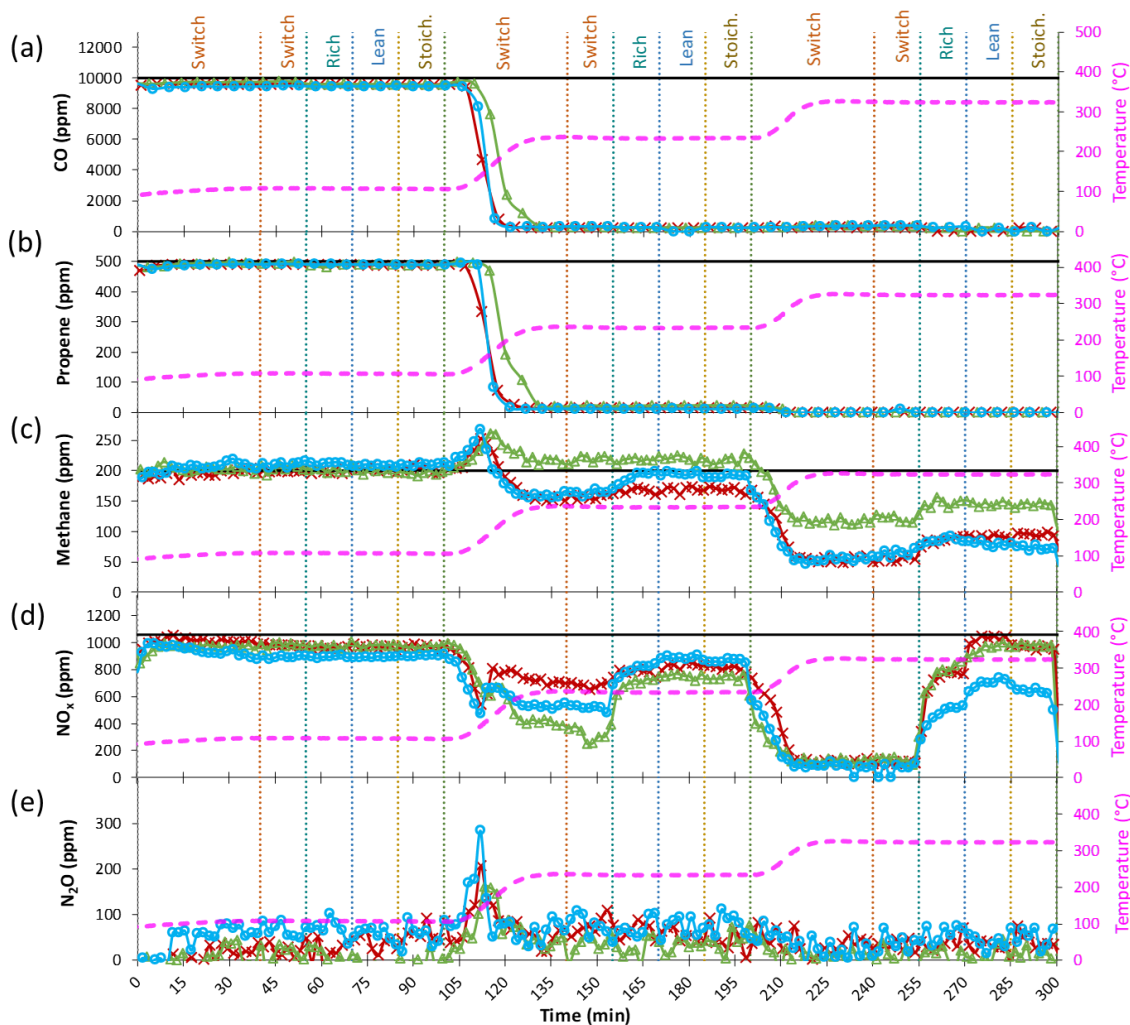


Fig. 2 Outlet concentration profiles of (a) CO, (b) C₃H₆, (c) CH₄, (d) NO_x and (e) N₂O during temperature-programmed catalytic testing in a complex mixture composition with Monolith-A-full (red crosses), Monolith-A-front (blue circles), Monolith-A-back (green triangles) under switch (1s lean/rich), rich, lean and stoichiometric conditions. The deep black lines represent the initial concentration of each gaseous reactant

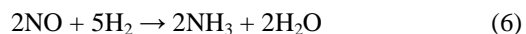
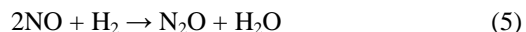
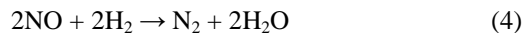
3.2.2. Catalyst pre-heating against N₂O formation

Among strategy for reducing pollution during cold-start, installation of an external pre-heating step of the catalyst up to a sufficiently high temperature has been envisaged such that N₂O formation can be efficiently minimized. To examine the optimum pre-heating temperature, Monolith-A-full and Monolith-A-back catalysts have been exposed to the complex mixture gas composition at every 50 °C under the lean/rich transient mode in which the NO conversion was found to be optimal. At high temperature above 300°C, Figure 3 (Monolith-A-full) and Figure 4 (Monolith-A-back) show that both catalysts converge to the same catalytic behavior with a quasi-full conversion of NO to nitrogen. Incomplete NO reduction with parallel production of N₂O is mainly observed below 250°C and notably at 150°C. Interestingly only the first half of the profile for Monolith-A-full at 150 °C favors NO reduction by CO to N₂O according to Eq (1). In principle, N₂O can be subsequently reduced to nitrogen according to Eq (3). A

strong discontinuity appears with a strong loss of NO conversion (Figure 3c) while CO and C₃H₆ become quasi-converted. Such observation emphasizes the occurrence of the competitive CO oxidation by O₂ according to Eq (2). Hence, CO would be no longer available for the reduction of NO.



The same discontinuity was not observed in the case of Monolith-A-back at 150 °C where CO and C₃H₆ are still present in high concentrations. Indeed, complete oxidation reactions are only observed at higher temperature of 250°C (Figure 4a and 4b). This is not surprising owing to the lower Pd concentration in Monolith-A-back. At 150 °C, around 1000 ppm of CO are missing in the gas feed that certainly correspond to the 500 ppm conversion of NO to form N₂O then N₂ according to Eqs (1) and (3). It is worth to note that some NO conversion could account for reduction by H₂ at this temperature to form N₂, N₂O or NH₃ according to following equations. H₂ profiles (not reported here) show complete conversion at 150 °C and a small spike of ammonia is recorded at the same temperature (Figure S3).



Finally, NO and CO conversion temperatures for both monoliths are consistent with those observed during temperature programmed catalytic tests in switch regimes (Figure 2). Pre-heating the catalyst does not affect its performance for better or worse, however, these outcomes highlight that a pre-heating temperature of 300 °C is necessary to avoid residual trace amount of N₂O in the exhaust during the cold start engine, in line with previous findings [35].

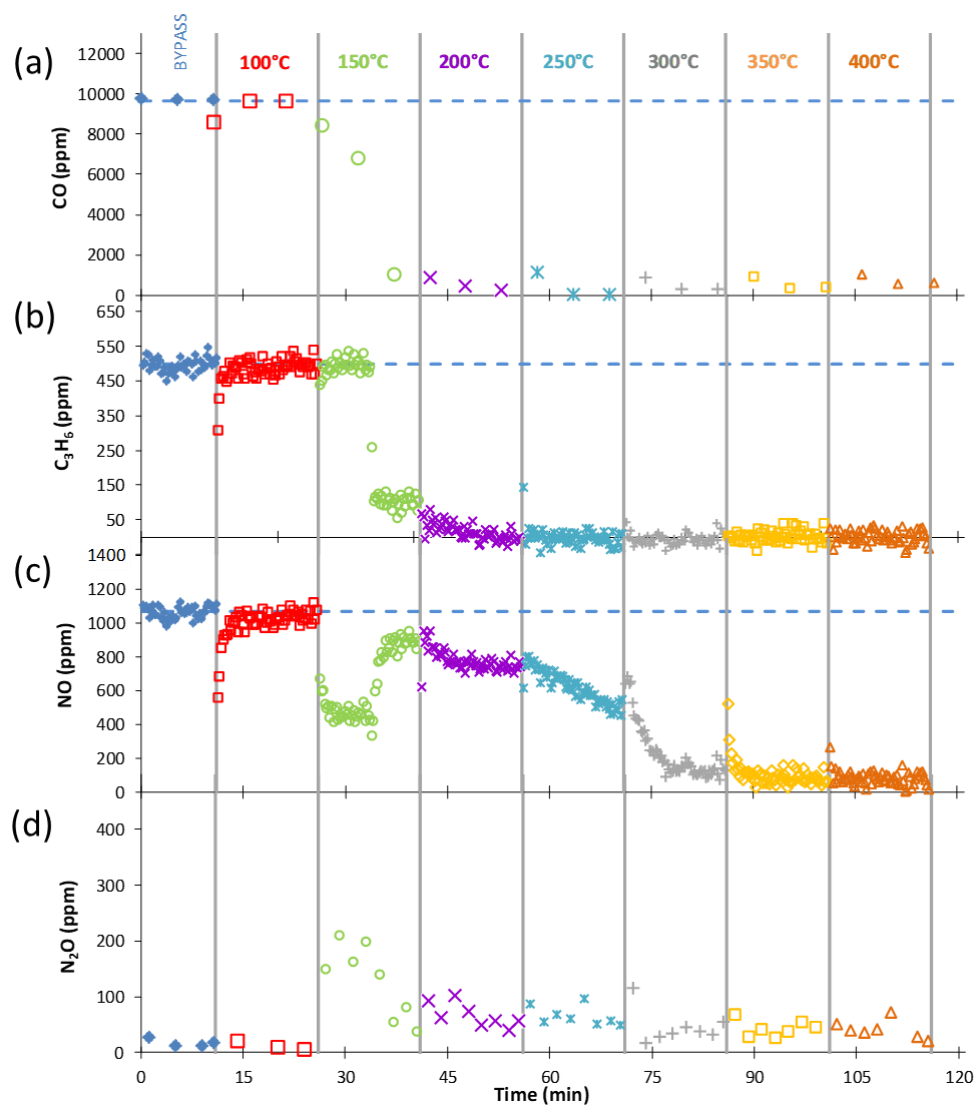


Fig. 3 Exposure of Monolith-A-full to the mixture gas at different temperatures during 1s lean/rich transient regime showing outlet profiles of (a) CO, (b) C₃H₆, (c) NO and (d) N₂O. Each vertical line represents the catalyst was subjected to O₂/He environment between every temperature interval while dotted blue horizontal lines represent the initial concentration of CO, C₃H₆ and NO reactants

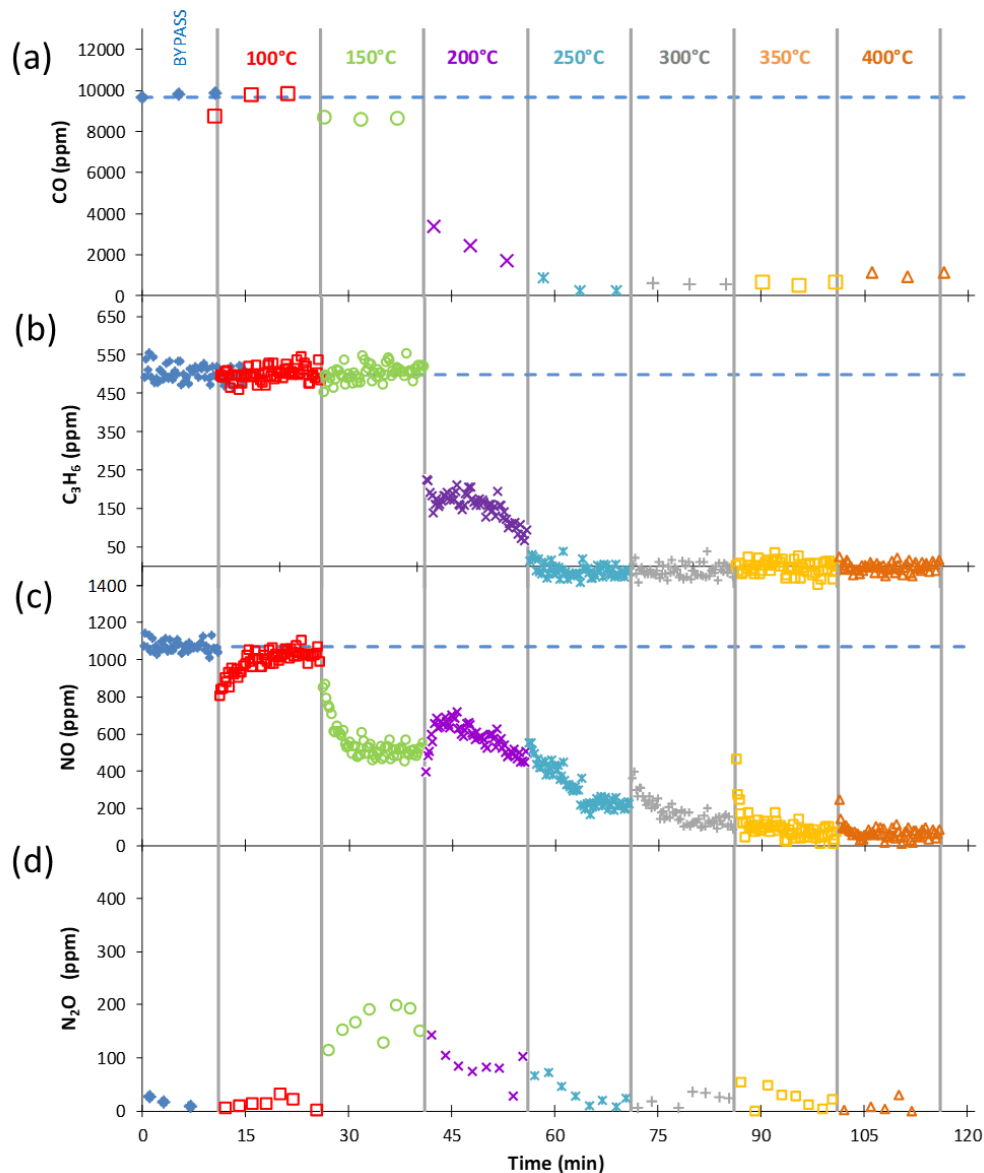


Fig. 4 Exposure of Monolith-A-back to the mixture gas at different temperatures during 1s lean/rich transient regime showing outlet profiles of (a) CO, (b) C_3H_6 , (c) NO and (d) N_2O . Each vertical line represents the catalyst was subjected to O_2/He environment between every temperature interval while dotted blue horizontal lines represent the initial concentration of CO, C_3H_6 and NO reactants

The pre-heating strategy is further examined by performing a catalytic test at the chosen temperature of $300^\circ C$ by direct exposure to the complex mixture under varying regimes as shown in Figure 5. The catalysts are initially under the rich conditions (rich1) followed by switch, rich2, lean, stoichiometric and switch2 regimes. This allows inspecting the behavior of the catalyst under variable air-to-fuel ratios as well as the impact of the order of the regimes, if any. Remarkably, NO conversion for Monolith-A-full displayed in Figure 5(a) reaches 71% or twice more than in rich2 mode (33%) during rich1 regime. No such difference is observed for Monolith-A-back catalyst where only 20% of NO conversion is obtained at steady-state in both rich modes. Moreover, the two successive

switch modes show similar behavior i.e. almost full NO conversion for both monoliths confirming the best catalytic performances obtained during transient 1s lean/rich regime. Interestingly, these observations can be transposed to some extent to the evolution of methane concentration in the different air-to-fuel ratios. Best performances are reached during transient modes for both catalysts while rich1 regime on Monolith-A-full shows a slightly better CH₄ conversion than rich2 (68% vs. 59% respectively), which is not observed with the back monolith part. Regarding the N₂O formation we can observe in Figure 5(b) that this pre-heating step certainly avoids the N₂O formation, and remains such under the change of the regimes as well.

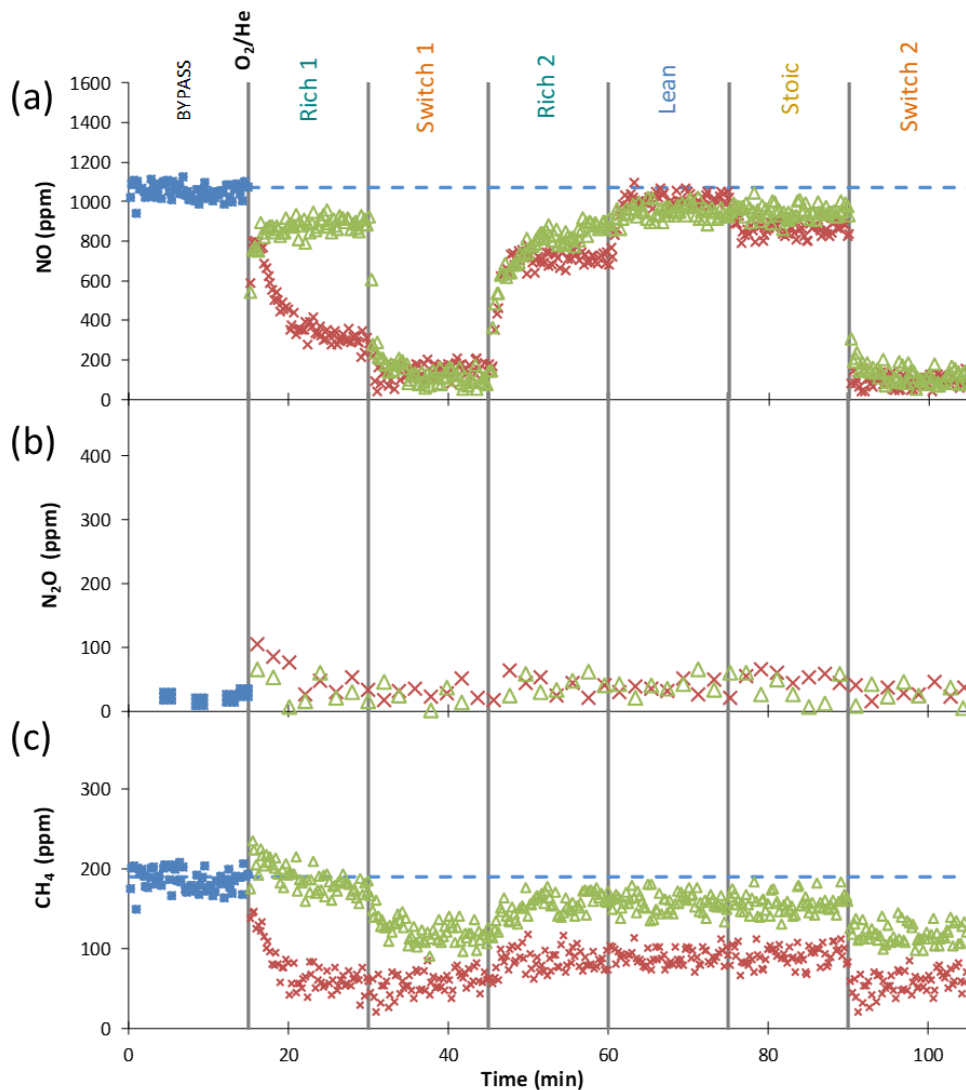


Fig. 5 Exposure of Monolith-A-full (red crosses) and Monolith-A-back (green triangles) to mixture gas composition on pre-heating the catalysts at 300°C: Concentration profiles of (a) NO, (b) N₂O and (c) CH₄ under different regimes rich1, switch1, rich2, lean, stoichiometric, switch2. Dotted blue lines represent the initial concentration of NO and CH₄ reactants

3.3 General assessment

The two technological strategies for minimizing typical cold-start emissions like N₂O by (i) catalyst designing through zone-coating with exceptionally high Pd loadings and (ii) catalyst pre-heating to intermediate temperatures helped to evaluate their present and future commercial validation. The unusually high Pd loading by zone coating was not successful in avoiding cold start emissions. In this case, N₂O formation is still prevalent at low temperatures. Simply higher Pd loadings do not improve catalytic performances beyond a certain concentration of such precious metals [36–38] since strong CO and Pd interactions can occur making desorption of CO from Pd a rate-limiting step [39]. Rapid rates of oxidation are also observed on catalyst exhibiting a high density of Pd active sites, leading to an insufficient concentration of CO, HC and H₂ which are required for NO_x reduction [40]. In addition, high Pd loading favors high-temperature sintering besides also increasing the manufacturing cost of such catalysts. On the other hand, pre-heating seems a better option and highly efficient method in regards to avoiding N₂O cold start emission, as seen in previous studies as well, while maintaining similar catalytic performances [1, 41]. One might conceivably point out that preheating strategy consumes higher energy derived through higher fuel consumption.

Beyond N₂O emissions, high catalytic performance for both oxidation and reduction reactions under the transient switch mode at low temperature is evidenced. It is noteworthy to see that in each case, especially at 200 °C and 300 °C, a higher catalytic activity for NO_x reduction and methane oxidation can be distinguished during the 1s lean/rich transient mode, while the impact of the steady-state regimes (lean, rich and stoichiometric) on the concentration profiles is less significant. Similar performances under all the steady-state conditions were observed earlier for the model CO and propene oxidation reactions for the same catalyst in our previous work and was attributed to the enhanced OSC properties of this monolithic catalyst [27]. It may be considered that during the transient condition the catalyst active species can experience change in their oxidation state and structure, which can dramatically impact the conversion rates. Some studies showed that mixed PdO_x (metal-ionic sites) species can be more active than the PdO (fully oxidized sites) ones for methane oxidation, the occurrence of which primarily depends on the variation of the oxygen feed subjected to the catalyst that can be maintained through a periodic lean/rich environment close to stoichiometric operating conditions [42–46]. Along similar lines, the respective orders of the regimes also have an influence as evidenced by the differences on NO outlet concentrations in rich1 and rich2 regimes. It is most probably resulting from difference of catalytic active surface sites before and after exposing to the mixed compositions of gases. To investigate this, a feasible approach would be to study the catalyst surface evolution by XPS after exposure to the pollutants by quasi *in situ* analysis and/or by *in situ* XAS analysis. However, this would remain the scope of another study. Finally, it is worth mentioning that the introduction of a large amount of water in the gas feed could have a significant impact on the result reported in this work by promoting reforming or reverse water-gas-shift reactions. The latter are obviously not prevalent here where water is assumed to be formed in only trace amount.

4. Conclusions

A commercial three-way catalyst and its different coating zones currently used by a major car manufacturer have been investigated in this paper for, firstly, assessing the impact of the zone-coating on it and, secondly, the effectiveness of incorporating a catalyst pre-heating step under transient lean/rich mode during cold-start conditions, referred to as the switch regime in this work. It was evidenced that the occurrence of increasing the PGM loading through zone coating allows combining improved catalytic conversion of CO and HC oxidation due to high Pd loading as well as improved NO reduction thanks to higher Rh loading on the back side. However, no important beneficial effect was observed in this case for avoiding N₂O formation at lower temperatures of up to 200 °C. The pre-heating of catalyst at 300 °C was on the other hand shown to be highly effective for preventing N₂O from forming. Interestingly, in all cases the transient mode was revealed to be the most active regime at all temperature ranges of the current study.

The results reported in this study will provide directions to optimize the PGM concentration in regards of pre-heating strategy and cost/performances ratio for further development of three-way catalysts keeping in mind the cold start emission challenge and new pollutant thresholds (N₂O, CH₄, NH₃) from European regulations.

References

1. Gao J, Tian G, Sornioti A, et al (2019) Review of thermal management of catalytic converters to decrease engine emissions during cold start and warm up. *Applied Thermal Engineering* 147:177–187. <https://doi.org/10.1016/j.applthermaleng.2018.10.037>
2. Farrauto RJ, Deeba M, Alerasool S (2019) Gasoline automobile catalysis and its historical journey to cleaner air. *Nature Catalysis* 2:603–613. <https://doi.org/10.1038/s41929-019-0312-9>
3. Martínez-Arias A, Fernández-García M, Hungria AB, et al (2001) Effect of Thermal Sintering on Light-Off Performance of Pd/(Ce,Zr)Ox/Al₂O₃ Three-Way Catalysts: Model Gas and Engine Tests. *Journal of Catalysis* 204:238–248. <https://doi.org/10.1006/jcat.2001.3379>
4. Rood S, Eslava S, Manigrasso A, Bannister C (2020) Recent advances in gasoline three-way catalyst formulation: A review. *Proceedings of the Institution of Mechanical Engineers, Part D: Journal of Automobile Engineering* 234:936–949. <https://doi.org/10.1177/0954407019859822>
5. González-Marcos MP, Pereda-Ayo B, Aranzabal A, et al (2012) On the effect of reduction and ageing on the TWC activity of Pd/Ce 0.68Zr 0.32O₂ under simulated automotive exhausts. *Catalysis Today* 180:88–95. <https://doi.org/10.1016/j.cattod.2011.04.035>
6. Lafyatis DS, Ballinger TH, Lammey G, et al (1998) Ambient temperature light-off aftertreatment system for meeting ULEV emission standards. *SAE Technical Papers* 980421. <https://doi.org/10.4271/980421>
7. Cominos V, Gavriilidis A (2001) An Experimental Study of Non-Uniform Pd Catalytic Monoliths. *Chemical Engineering Research and Design* 79:795–798. <https://doi.org/10.1205/026387601753191975>
8. Gandhi HS, Graham GW, McCabe RW (2003) Automotive exhaust catalysis. *Journal of Catalysis* 216:433–442. [https://doi.org/10.1016/S0021-9517\(02\)00067-2](https://doi.org/10.1016/S0021-9517(02)00067-2)
9. Wang J, Chen H, Hu Z, et al (2015) A Review on the Pd-Based Three-Way Catalyst. *Catalysis Reviews* 57:79–144. <https://doi.org/10.1080/01614940.2014.977059>
10. Heck RM, Gulati S, Farrauto RJ (2001) The application of monoliths for gas phase catalytic reactions. *Chemical Engineering Journal* 82:149–156. [https://doi.org/10.1016/S1385-8947\(00\)00365-X](https://doi.org/10.1016/S1385-8947(00)00365-X)
11. Tomašić V, Jović F (2006) State-of-the-art in the monolithic catalysts/reactors. *Applied Catalysis A: General* 311:112–121. <https://doi.org/10.1016/j.apcata.2006.06.013>
12. Govender S, Friedrich HB (2017) Monoliths: A Review of the Basics, Preparation Methods and Their Relevance to Oxidation. *Catalysts* 7:62. <https://doi.org/10.3390/catal7020062>
13. Papavasiliou A, Tsetsekou A, Matsouka V, et al (2009) Development of a Ce-Zr-La modified Pt/ γ -Al₂O₃ TWCs' washcoat: Effect of synthesis procedure on catalytic behaviour and thermal durability. *Applied Catalysis B: Environmental* 90:162–174. <https://doi.org/10.1016/j.apcatb.2009.03.006>
14. Papavasiliou A, Tsetsekou A, Matsouka V, et al (2010) An investigation of the role of Zr and La dopants into Ce_{1-x-y}Zr_xLa_yO₈ enriched γ -Al₂O₃ TWC washcoats. *Applied Catalysis A: General* 382:73–84. <https://doi.org/10.1016/j.apcata.2010.04.025>
15. Lang W, Laing P, Cheng Y, et al (2017) Co-oxidation of CO and propylene on Pd/CeO₂-ZrO₂ and Pd/Al₂O₃ monolith catalysts: A light-off, kinetics, and mechanistic study. *Applied Catalysis B: Environmental* 218:430–442. <https://doi.org/10.1016/j.apcatb.2017.06.064>
16. Bedrane S, Descorme C, Duprez D (2002) Investigation of the oxygen storage process on ceria- and ceria-zirconia-supported catalysts. *Catalysis Today* 75:401–405. [https://doi.org/10.1016/S0920-5861\(02\)00089-5](https://doi.org/10.1016/S0920-5861(02)00089-5)

17. Li J, Liu X, Zhan W, et al (2016) Preparation of high oxygen storage capacity and thermally stable ceria–zirconia solid solution. *Catal Sci Technol* 6:897–907. <https://doi.org/10.1039/C5CY01571E>
18. Li P, Chen X, Li Y, Schwank JW (2019) A review on oxygen storage capacity of CeO₂-based materials: Influence factors, measurement techniques, and applications in reactions related to catalytic automotive emissions control. *Catalysis Today* 327:90–115. <https://doi.org/10.1016/j.cattod.2018.05.059>
19. Konsolakis M, Yentekakis IV (2001) The reduction of NO by propene over Ba-promoted Pt/γ-Al₂O₃ catalysts. *Journal of Catalysis* 198:142–150. <https://doi.org/10.1006/jcat.2000.3123>
20. Kobayashi T, Yamada T, Kayano K (2001) Effect of basic metal additives on NO_x reduction property of Pd-based three-way catalyst. *Applied Catalysis B: Environmental* 30:287–292. [https://doi.org/10.1016/S0926-3373\(00\)00240-X](https://doi.org/10.1016/S0926-3373(00)00240-X)
21. Zhao B, Wang Q, Li G, Zhou R (2013) Effect of rare earth (La, Nd, Pr, Sm and Y) on the performance of Pd/Ce_{0.67}Zr_{0.33}MO_{2-δ} three-way catalysts. *Journal of Environmental Chemical Engineering* 1:534–543. <https://doi.org/10.1016/j.jece.2013.06.018>
22. Haneda M, Tomida Y, Sawada H, Hattori M (2016) Effect of Rare Earth Additives on the Catalytic Performance of Rh/ZrO₂ Three-Way Catalyst. *Topics in Catalysis* 59:1059–1064. <https://doi.org/10.1007/s11244-016-0590-2>
23. Favez J-Y, Weilenmann M, Stilli J (2009) Cold start extra emissions as a function of engine stop time: Evolution over the last 10 years. *Atmospheric Environment* 43:996–1007. <https://doi.org/10.1016/j.atmosenv.2008.03.037>
24. Chang H-L, Chen H-Y, Koo K, et al (2014) Gasoline Cold Start Concept (gCSCTM) Technology for Low Temperature Emission Control. *SAE Int J Fuels Lubr* 7:480–488. <https://doi.org/10.4271/2014-01-1509>
25. Mahadevan G, Subramanian S (2017) Experimental Investigation of Cold Start Emission using Dynamic Catalytic Converter with Pre-Catalyst and Hot Air Injector on a Multi Cylinder Spark Ignition Engine. *SAE Technical Paper* 2017-01-2367. <https://doi.org/10.4271/2017-01-2367>
26. Kodyath R, Tanaka H, Nagao Y, et al (2019) Controlled Distribution of PGM in Transversal and Vertical Direction of Washcoat; New Approach for Targeting Emission at Cold Start and High Speed Region. *SAE Technical Paper* 2019-26-0144. <https://doi.org/10.4271/2019-26-0144>
27. Nandi S, Arango P, Chaillou C, et al (2022) Relationship between design strategies of commercial three-way monolithic catalysts and their performances in realistic conditions. *Catalysis Today* 384–386:122–132. <https://doi.org/10.1016/J.CATTOD.2021.05.005>
28. He L, Fan Y, Bellettre J, et al (2020) A review on catalytic methane combustion at low temperatures: Catalysts, mechanisms, reaction conditions and reactor designs. *Renewable and Sustainable Energy Reviews* 119:109589. <https://doi.org/10.1016/J.RSER.2019.109589>
29. Haneda M, Shinoda K, Nagane A, et al (2008) Catalytic performance of rhodium supported on ceria–zirconia mixed oxides for reduction of NO by propene. *Journal of Catalysis* 259:223–231. <https://doi.org/10.1016/j.jcat.2008.08.007>
30. Yoshida H, Koizumi K, Boero M, et al (2019) High Turnover Frequency CO–NO Reactions over Rh Overlayer Catalysts: A Comparative Study Using Rh Nanoparticles. *J Phys Chem C* 123:6080–6089. <https://doi.org/10.1021/acs.jpcc.9b00383>
31. Kibis LS, Svintsitskiy DA, Derevyannikova EA, et al (2019) From highly dispersed Rh³⁺ to nanoclusters and nanoparticles: Probing the low-temperature NO+CO activity of Rh-doped CeO₂ catalysts. *Applied Surface Science* 493:1055–1066. <https://doi.org/10.1016/j.apsusc.2019.07.043>

32. Holles JH, Davis RJ, Murray TM, Howe JM (2000) Effects of Pd Particle Size and Ceria Loading on NO Reduction with CO. *Journal of Catalysis* 195:193–206. <https://doi.org/10.1006/jcat.2000.2985>
33. Williamson WB, Richmond RP, Nunan JG, et al (2001) Palladium and Platinum/Rhodium Dual-Catalyst NLEV and Tier IIA Close-Coupled Emission Solutions. SAE Technical Paper 2001-01-0923. <https://doi.org/10.4271/2001-01-0923>
34. Reddy GK, Ling C, Peck TC, Jia H (2017) Understanding the chemical state of palladium during the direct NO decomposition – influence of pretreatment environment and reaction temperature. *RSC Adv* 7:19645–19655. <https://doi.org/10.1039/C7RA00836H>
35. Dasch JM (1992) Nitrous Oxide Emissions from Vehicles. *Journal of the Air & Waste Management Association* 42:63–67. <https://doi.org/10.1080/10473289.1992.10466971>
36. Kang SB, Han SJ, Nam SB, et al (2012) Activity function describing the effect of Pd loading on the catalytic performance of modern commercial TWC. *Chemical Engineering Journal* 207–208:117–121. <https://doi.org/10.1016/j.cej.2012.06.003>
37. Phan DQ, Kureti S (2017) CO Oxidation on Pd/Al₂O₃ Catalysts under Stoichiometric Conditions. *Top Catal* 60:260–265. <https://doi.org/10.1007/s11244-016-0608-9>
38. Theis JR, Getsoian A (Bean), Lambert CK (2018) The Development of Low Temperature Three-Way Catalysts for High Efficiency Gasoline Engines of the Future: Part II. SAE Technical Paper 2018-01-0939. <https://doi.org/10.4271/2018-01-0939>
39. Martínez-Arias A, Hungría AB, Fernández-García M, et al (2004) Light-off behaviour of PdO/γ-Al₂O₃ catalysts for stoichiometric CO–O₂ and CO–O₂–NO reactions: a combined catalytic activity–in situ DRIFTS study. *Journal of Catalysis* 221:85–92. [https://doi.org/10.1016/S0021-9517\(03\)00277-X](https://doi.org/10.1016/S0021-9517(03)00277-X)
40. Brisley RJ, Chandler GR, Jones HR, et al (1995) The Use of Palladium in Advanced Catalysts. SAE Technical Paper 950259. <https://doi.org/10.4271/950259>
41. Vilwanathan Velmurugan D, McKelvey T, Olsson J-O (2022) Data-Driven Near-Optimal On-Line Control for an Electrically Heated Catalyst-Equipped Gasoline Engine. *SAE Int J Engines* 16:. <https://doi.org/10.4271/03-16-03-0019>
42. Carlsson P-A, Fridell E, Skoglundh M (2007) Methane oxidation over Pt/Al₂O₃ and Pd/Al₂O₃ catalysts under transient conditions. *Catal Lett* 115:1–7. <https://doi.org/10.1007/s10562-007-9057-1>
43. Grunwaldt J-D, Vegten N van, Baiker A (2007) Insight into the structure of supported palladium catalysts during the total oxidation of methane. *Chem Commun* 44:4635–4637. <https://doi.org/10.1039/B710222D>
44. Petrov AW, Ferri D, Krumeich F, et al (2018) Stable complete methane oxidation over palladium based zeolite catalysts. *Nat Commun* 9:1–8. <https://doi.org/10.1038/s41467-018-04748-x>
45. Franken T, Roger M, Petrov AW, et al (2021) Effect of Short Reducing Pulses on the Dynamic Structure, Activity, and Stability of Pd/Al₂O₃ for Wet Lean Methane Oxidation. *ACS Catal* 11:4870–4879. <https://doi.org/10.1021/acscatal.1c00328>
46. Wang M, Dimopoulos Eggenschwiler P, Franken T, et al (2021) Reaction pathways of methane abatement in Pd-Rh three-way catalyst in heavy duty applications: A combined approach based on exhaust analysis, model gas reactor and DRIFTS measurements. *Chemical Engineering Journal* 422:129932. <https://doi.org/10.1016/j.cej.2021.129932>